Temperature Dependence and Fracture Criterion of Mixed Mode I/II Fracture Toughness of Phenolic Resin for Friction Material

Wakako Araki,[1] Hiroki Shintaku,[1] Hiroyuki Ohashi,[2] Yoshiki Horiuchi,[2] Yoshio Arai[1]

[1]*Department of Mechanical Engineering, Saitama University, Sakura-ku, Saitama 338 8570, Japan*
[2]*Department of Engineering, Tochigi Nisshin, Nogi-machi, Shimotsuga-gun, Tochigi 329 0114, Japan*

Received 16 June 2010; accepted 11 December 2010
DOI 10.1002/app.33939
Published online 16 March 2011 in Wiley Online Library (wileyonlinelibrary.com).

ABSTRACT: In this study, the temperature dependence of the mixed-mode fracture toughness of the phenolic resin for friction materials is investigated. For pure mode I, the fracture toughness decreases as the temperature increases, and it increases again after showing its minimum value. For pure mode II, the fracture toughness shows a similar trend but has its minimum value at a higher temperature. The temperature dependence of the mixed-mode fracture toughness varies depending on the mode mixity, which is attributed to the different sensitivity to the relaxation phenomenon. At room temperature, as the fracture toughness for pure mode I and II are almost the same, the fracture locus shows a circular arc. At elevated temperatures, the locus becomes smaller and noncircular. At high temperature, the fracture locus shows an elliptical arc, where the fracture toughness for pure mode II is smaller than that for mode I. An empirical fracture criterion based on the time-temperature dependence of the resin is proposed, and the proposed method successfully predicts the fracture toughness under various conditions of the temperature, time, and mode mixity. The crack initiation angles, on the other hand, are almost consistent regardless of the temperature, which agree with the maximum hoop stress theory. © 2011 Wiley Periodicals, Inc. J Appl Polym Sci 121: 2301–2309, 2011

Key words: mixed mode fracture; fracture toughness; phenolic resin; viscoelasticity

INTRODUCTION

As the phenolic resin has good mechanical, electrical, adhesive, and thermal properties, it has been used in various engineering fields. Rubber-modified phenolic resin is widely used as friction materials for brake pads and linings of automobiles and trains by combining tens of inorganic fillers, fibres, and particles to achieve high friction and wear coefficients in a wide range of temperature and pressure.[1–3] In addition to those properties, high fracture toughness is a very important factor for the safety.

The phenolic resin is generally known as a thermo-viscoelastic material, elastic modulus of which greatly depends on time and also temperature due to relaxation phenomena. Both time and temperature dependences can be taken into account by the time-temperature equivalent principle.[4] It has been reported that other mechanical properties such as yield stress, strength, and fracture toughness also have strong time-temperature dependences, where the time-temperature equivalent principle is still applicable to those properties.[5–9] As for the fracture toughness, several studies have obtained the time-temperature dependence of mode I fracture toughness, whereas there are few researches on that of mode II and mixed mode I/II fracture toughness.[9–16] Our previous studies[13,17] have shown that the mode I and II fracture toughness of the epoxy resin have different time-temperature dependences, indicating that the conventional fracture criteria would be unavailable for the thermo-viscoelastic materials. Although the time and/or rate dependence of the fracture toughness have been observed in the literatures, any practical fracture criterion that considers the time-temperature dependence of the mixed-mode fracture toughness of the thermo-viscoelastic materials has not been proposed so far.

In this study, the fracture toughness of the phenolic resin for friction materials is examined under various conditions of the temperature and mode mixity to investigate the temperature dependence of the mixed-mode I/II fracture toughness. An empirical fracture criterion is proposed based on the experimental results.

EXPERIMENT

In this study, rubber-modified phenolic resin for friction materials (Sumiliteresin®PR Series, Sumitomo

Correspondence to: W. Araki (araki@mech.saitama-u.ac.jp).

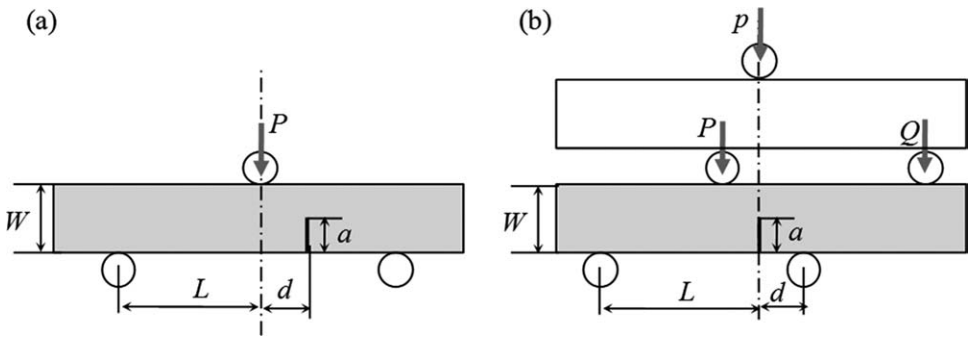

Figure 1 Geometry of specimens for (a) 3PBT and (b) 4PBT.

Bakelite), which contains hexamine, is investigated. The resin powders were moulded and cured at 433 K for 1 h under an appropriate pressure. Then, the specimens with the size of 60 × 10 × 5 mm^3 were cut out from the plate. It should be noted that the geometry was confirmed to satisfy the plain strain condition.

The three- and four-point bending tests (3PBT and 4 PBT) were conducted to examine the mixed-mode I/II fracture toughness.[17–21] The geometry and the size of the specimens are shown in Figure 1 and Table I, respectively. The stress field around the crack can be changed by the distance from the centre to the crack d in the 3PBT and by the precrack length a in the 4PBT. The stress intensity factors, K_I and K_{II}, are given by:

$$K_I = \sigma_0 F_I \sqrt{\pi a} \tag{1}$$

$$K_{II} = \sigma_0 F_{II} \sqrt{\pi a} \tag{2}$$

where F_I, F_{II}, and σ_0 for the 3PBT are:

$$\sigma_0 = \frac{3PL}{W^2 B}$$

$$F_I = F_{I3}\left(1 - \frac{a}{W}\right)^{\frac{3}{2}}$$

$$F_{II} = F_{II3}\left(1 - \frac{a}{W}\right)^{\frac{1}{2}}$$

and those for the 4PBT are:

$$\sigma_0 = \frac{P}{WB}$$

$$F_I = F_{I4}\left(1 - \frac{d}{W}\right)$$

$$F_{II} = F_{II4}\left(1 - \frac{d}{W}\right)$$

$$P = \frac{L}{L+d}p, \quad Q = \frac{d}{L+d}p$$

where L, W, B, and a are the length, width, thickness of the sample, and the initial crack length, respectively, and d and p are explained in the Figure 1. F_{I3}, F_{II3}, F_{I4}, and F_{II4} are geometric functions given in Refs. 19,20. By substituting the maximum load at fracture P_c into P in eqs. (1) and (2), the mode I and II components of the fracture toughness, $(K_I)_c$ and $(K_{II})_c$, were determined.

As the stress field around the crack tip is subjected to the mixed mode loading, the mode mixity parameter ϕ is used:

$$\phi = \frac{2}{\pi}\tan^{-1}\left(\frac{K_{II}}{K_I}\right) \tag{3}$$

In this study, the mode mixity ϕ can be varied from 0 to 0.5 in the 3PBT and from 0.6 to 0.98 in the 4PBT, in which range the geometric functions are defined. The distance d was used so as to obtain ϕ = 0, 0.1, 0.2, 0.3, 0.4 in the 3PBT, whereas the random values of ϕ between 0.6 and 0.98 were used in the 4PBT because ϕ was very sensitive to the precrack length a.

All the fracture toughness tests were conducted in a furnace (170-500, Toshin Kogyo) by using a universal testing machine (666, MTS) with a loadcell (TCLA-1KNA, Tokyo Sokki). The displacement rate was 0.017 μm/s. The temperature was ranged from 298 to 380 K, which was measured at the surface of the specimen.

The dynamic mechanical analysis (DMS6000, EXSTAR600) was conducted to examine the dynamic storage and loss moduli, E' and E''. The bending mode was used and the frequency was 1, 5, and 10 Hz. The temperature was increased by 1 K/min from 298 to 573 K. The measurement was conducted in the nitrogen flow (250 mL/min).

TABLE I
Size of Specimen for 3PBT and 4PBT

	L (mm)	W (mm)	B (mm)	d (mm)	a (mm)
3PBT	20	10	5	0–18	5
4PBT	20	10	5	10	1–7

B, Thickness of the sample.

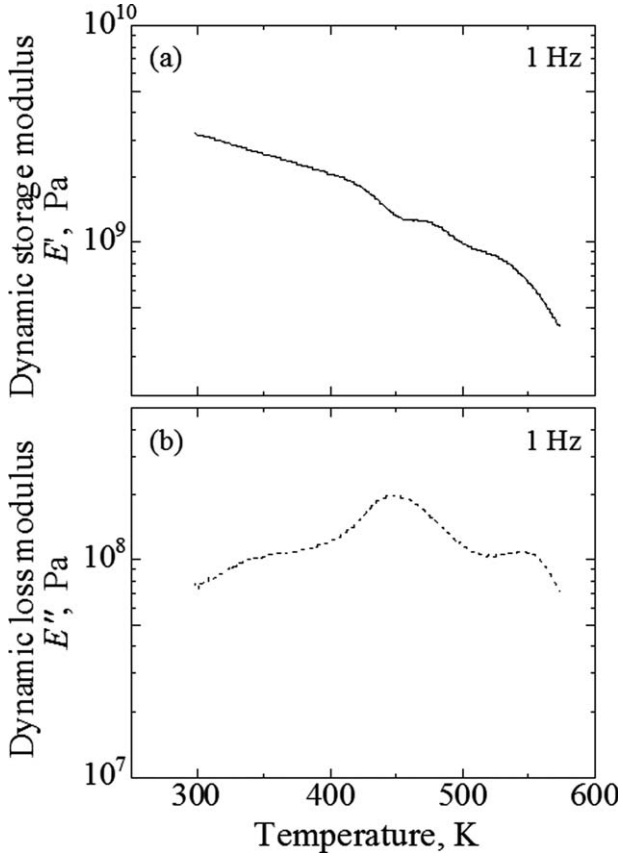

Figure 2 Dynamic storage (a) and loss moduli (b) measured at 1 Hz.

RESULTS AND DISCUSSION

Dynamic modulus

Figure 2 shows the dynamic storage modulus E' and loss modulus E'' measured at the frequency of 1 Hz from 298 to 573 K. The storage modulus E' at 298 K is about 3 GPa and gradually decreases as the temperature increases, and then it shows a distinct decrease around 430 K due to a glass transition of the phenolic resin, where probably the additional curing reaction is occurring around 450 K, followed by a drastic drop above 500 K due to the partial decomposition. The loss modulus E'' is around 0.08 GPa at 298 K and gradually increases from 300 to 400 K and peaks around 450 K when E' shows the distinct decrease.

It is widely known that the thermo-viscoelastic materials follow the time-temperature equivalent principle.[4] The shift factor a_T, i.e., the time-temperature equivalent factor, can be expressed as follows:

$$E'(T, \log\ t) = E'(T_{\mathrm{R}}, \log\ t - \log\ a_{\mathrm{T}}) = E'(T_{\mathrm{R}}, \log\ t_{\mathrm{R}}), \tag{4}$$

where t, T, T_R, and t_R are time, temperature, reference temperature, and reduced time, respectively. Figure 3 shows the shift factor a_T for $T_R = 298$ K derived from the temperature dependence of E' measured at different frequencies. The glass transition temperature T_g evaluated from the change of the slope in Figure 3 is 433 K in this study.[11] The shift factor a_T will be used to obtain master curves later in this article.

Fracture toughness

Figure 4 shows the load-displacement curves measured at the room temperature (298 K) under various mode mixities ϕ, where the displacement was measured at the loading points of P for 3PBT and p for 4PBT shown in Figure 1. All the specimens show a linear relationship and a brittle fracture. As ϕ increases, the fracture load P_c increases in the 3PBT, whereas it decreases in the 4PBT. Figure 5 shows the load-displacement curves measured at 380 K. The specimen for $\phi = 0$ shows a slightly ductile fracture (i.e., quasi-brittle fracture[11,13]), whereas the other specimens fracture in a brittle manner. The fracture toughness are determined from the maximum loads for both brittle and quasi-brittle cases in this study.

Figure 6 shows the fracture toughness $(K_{\mathrm{I}})_{\mathrm{c}}$ and $(K_{\mathrm{II}})_{\mathrm{c}}$ measured at 298 K under various mode mixities ϕ. The fracture toughness $(K_{\mathrm{I}})_{\mathrm{c}}$ monotonically decreases with increasing ϕ, whereas $(K_{\mathrm{II}})_{\mathrm{c}}$ increases, and $(K_{\mathrm{II}})_{\mathrm{c}}$ becomes higher than $(K_{\mathrm{I}})_{\mathrm{c}}$ for $\phi > 0.5$. Figure 7 shows the temperature dependence of the fracture toughness $(K_{\mathrm{I}})_{\mathrm{c}}$ and $(K_{\mathrm{II}})_{\mathrm{c}}$ for different mode mixities. For $\phi = 0$, i.e., pure mode I fracture case, the fracture toughness $(K_{\mathrm{I}})_{\mathrm{c}}$ is about 1.0 MPa $m^{1/2}$ at 298 K but decreases to 0.7 MPa $m^{1/2}$ up to about 320 K, but it increases

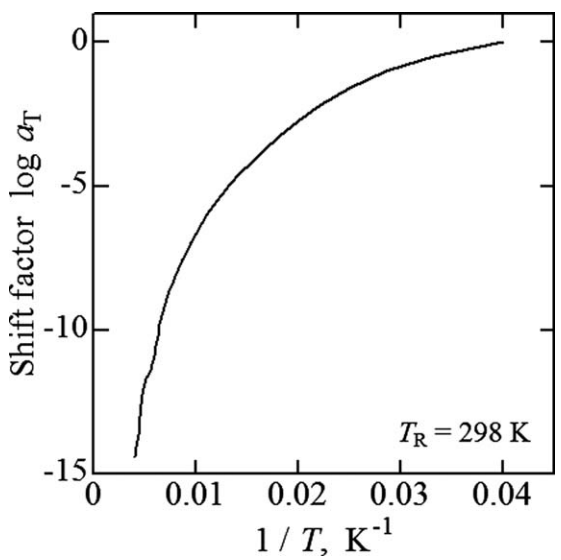

Figure 3 Shift factor.

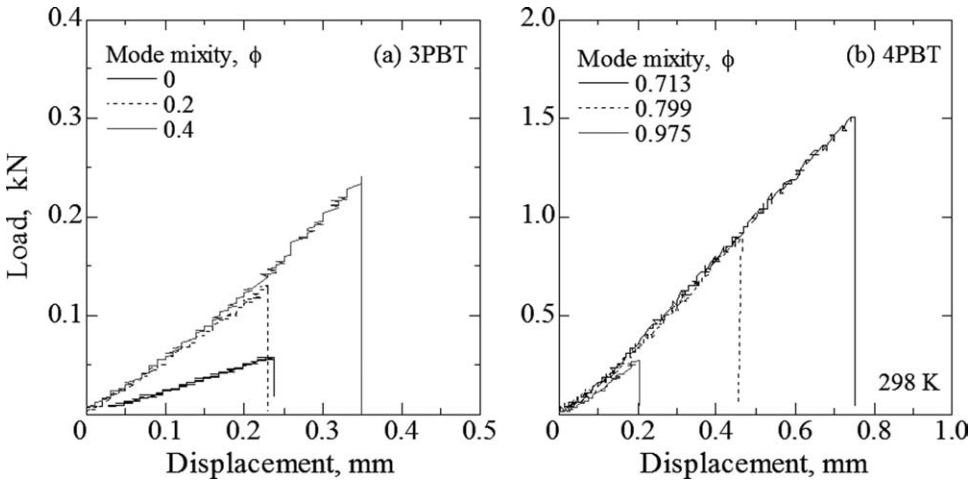

Figure 4 Load-displacement curves measured at 298 K.

again at higher temperatures. For $\phi = 0.2$, $(K_I)_c$ are generally smaller than those for $\phi = 0$, especially at lower temperatures, and there is no clear trend observed. For $0.62 < \phi < 0.72$, $(K_{II})_c$ are larger than $(K_I)_c$ and the minimum is observed around 340 K. For $0.96 < \phi < 0.98$, $(K_{II})_c$ decreases with increasing the temperature and has a minimum value around 360 K. These results clearly demonstrate that the mixed-mode fracture toughness depends on the temperature and also that the temperature dependence is varied by the mode mixity.

The fracture toughness for pure mode I and II, K_{Ic} and K_{IIc}, are summarized in Table II, where K_{Ic} is obtained by averaging the results for $\phi = 0$ and K_{IIc} is determined by the extrapolation of the results obtained for $\phi = 0.6$ to 0.98[17] because F_{II} in eq (2) has not been defined for $f = 1$.

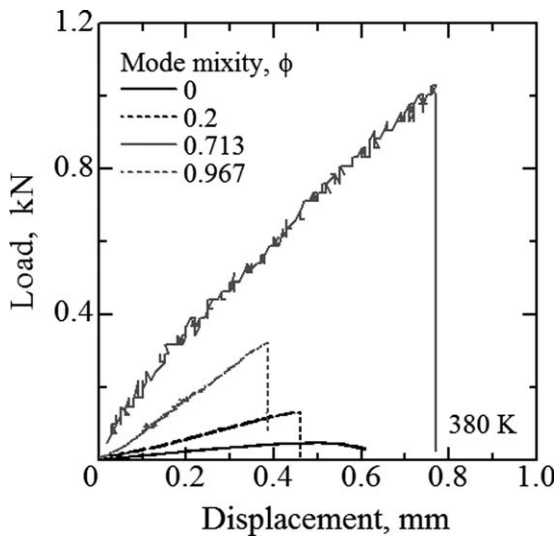

Figure 5 Load-displacement curves measured at 380 K.

Master curves of dynamic modulus and fracture toughness

Figure 8 shows the master curves of dynamic moduli E' and E'' with the fracture toughness $(K_I)_c$ for $\phi = 0$ and $(K_{II})_c$ for $0.96 < \phi < 0.98$ at the reference temperature T_R obtained by using the shift factor a_T in Figure 3, where the fracture time t_f is used to obtain the master curve of the fracture toughness.[11–13] The comparison of $(K_I)_c$ with $(K_{II})_c$ in Figure 8 is almost equivalent to that in Figure 7 because the fracture time t_f varies only between 10 and 50 s.

Both fracture toughness varies between 0.6 and 1.2 MPa·m$^{1/2}$ and they decrease with the reduced time t_R and increase again after their minimum values. The similar behaviors have been also reported for the epoxy resins and composites in our previous studies.[11,13] The decrease of the fracture toughness observed at shorter times (i.e., at lower temperatures) could be simply due to the decrease of the modulus as seen in the curve of E', whereas the increase of the toughness at longer times (i.e., at higher temperatures)

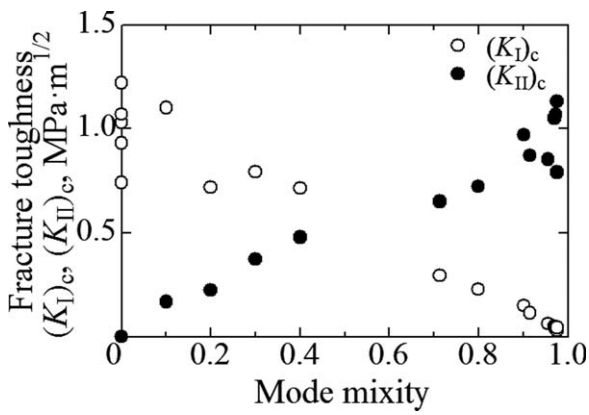

Figure 6 Mixed mode I/II fracture toughness measured at 298 K.

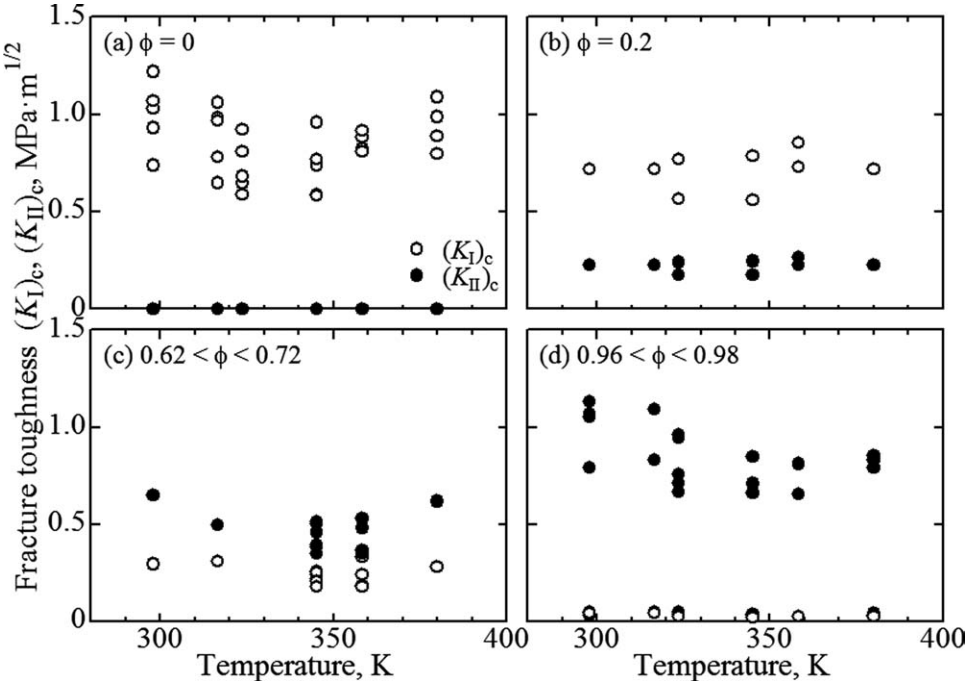

Figure 7 Temperature dependence of mixed mode I/II fracture toughness.

can be attributed to the increase of the viscosity caused by the relaxation phenomenon as seen in that of E'', which will lead to a brittle-ductile fracture transition in further long time (i.e., at further high temperature).[11,13] The minimum values of the fracture toughness are thus observed in between. Compared to the mode II fracture toughness, the mode I fracture toughness seems to be more easily affected by the relaxation phenomenon, resulting in the increase of the fracture toughness $(K_I)_c$ at the short time as seen in Figure 8 (or at the lower temperature as seen in Fig. 7) and also the quasi-brittle fractures at 380 K as shown in Figure 5. The different behaviors between mode I and II ($\phi = 0$ and 1) results in the complex behavior of the mixed-mode fracture toughness for $0 < \phi < 1.0$.

Application of conventional fracture criterion

Figure 9 shows the crack initiation angle $-\theta$ for various mode mixities with the prediction by the maximum hoop stress criterion (MHSC),[22] one of conventional fracture criteria, given by:

$$\tan\left(\frac{\theta}{2}\right) = \frac{K_I}{4K_{II}} \pm \frac{1}{4}\sqrt{\left(\frac{K_I}{K_{II}}\right)^2 + 8} \quad (5)$$

TABLE II
Pure Mode I and II Fracture Toughnesses

Temperature (K)	298	317	324	345	358	380
K_{Ic}, MPa m$^{1/2}$	1.01	0.910	0.713	0.699	0.853	0.938
K_{IIc}, MPa m$^{1/2}$	1.02	0.970	0.841	0.758	0.711	0.789

The angles at any temperatures almost agree each other and with the MHSC prediction, especially at higher temperatures.

Figure 10 shows the fracture locus $(K_I)_c - (K_{II})_c$ with the prediction by the MHSC given by:

$$\frac{1}{2}\cos\frac{\theta_c}{2}\{(K_1)_c(1+\cos\theta_c) - (K_{II})_c 3\sin\theta_c\} = K_{Ic} \quad (6)$$

where the values of K_{Ic} in Table II are used for the evaluation. The locus at 298 K shows a circular arc because K_{Ic} and K_{IIc} are almost the same values of 1.0 MPa m$^{1/2}$. The circle becomes smaller at 317 and 324 K. Then, the locus becomes larger again from 345 K, where the locus is no longer circular and very unstable, and it becomes an elliptic arc at

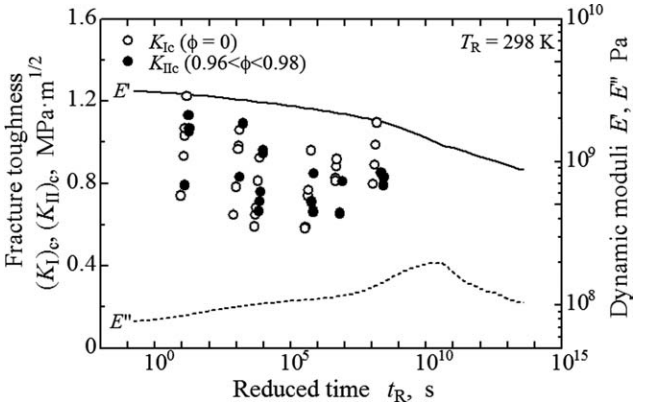

Figure 8 Master curves of dynamic moduli and fracture toughness.

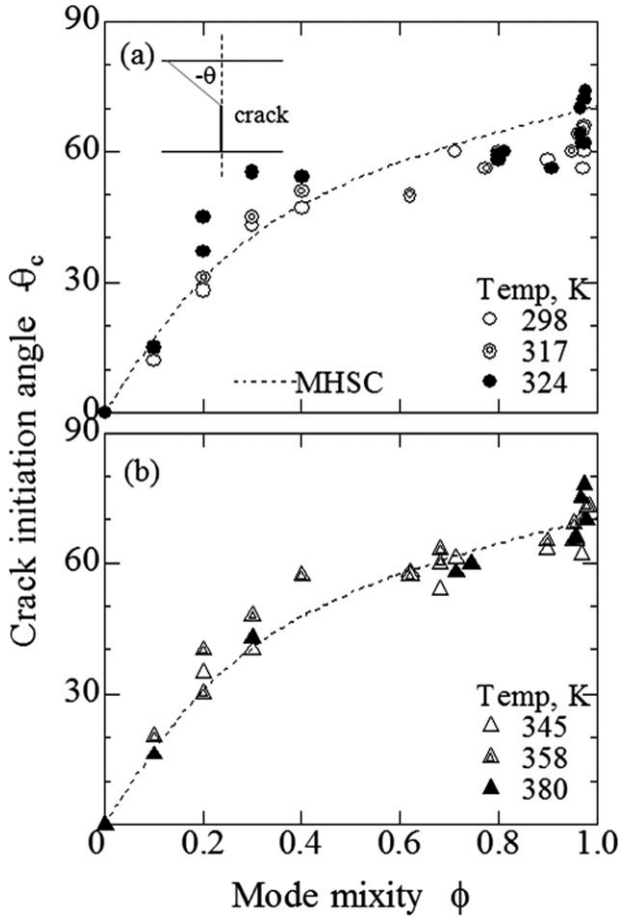

Figure 9 Crack initiation angle.

380 K, where K_{IIc} is smaller than K_{Ic}. The result is directly related to the different temperature dependence of the fracture toughness for different mode mixity as seen in Figures 7 and 8, indicating that the fracture criterion can be varied by the relaxation phenomenon whereas the MHSC gives a fixed circle. The similar results have been also discussed for the epoxy resins in our previous study.[13] The mixed mode fracture strongly affected by the relaxation cannot be predicted by any conventional fracture criteria such as the maximum hoop stress theory, the minimum strain energy density theory, and the maximum energy release rate theory, all of which can be determined only by K_{Ic} and generally give $K_{Ic}/K_{IIc} > 1$.

Therefore, the crack initiation angle can be simply determined by the stress state regardless of the relaxation phenomenon, whereas the fracture locus greatly changes depending on the temperature.

Proposal of empirical fracture criterion for viscoelastic materials

The mixed-mode fracture toughness of the viscoelastic materials shows a very complex behavior as seen in the previous chapters and also in the literatures, basically because the time-temperature dependence of the fracture toughness varies with the fracture mode, i.e., the mode mixity. Regardless of this complex behavior, the master curves of the pure mode I and II fracture toughness have generally a similar trend; both pure mode fracture toughness remain almost constant in the glassy region and, after showing a slight decrease, increase dramatically at the elevated temperature and then reach the maximum value around the brittle-ductile fracture transition.

Thus, the shape of the master curves are quite similar each other. When the master curve of the mode I fracture toughness K_{Ic} at the reference temperature T_R, e.g., Figure 8, is given by

$$K_{Ic} = K_{Ic}(\log\ t_R) = K_{Ic}\ (\tau_{RI}), \tag{7}$$

that of the mode II fracture toughness K_{IIc} can be then expressed by using K_{Ic} as follows:

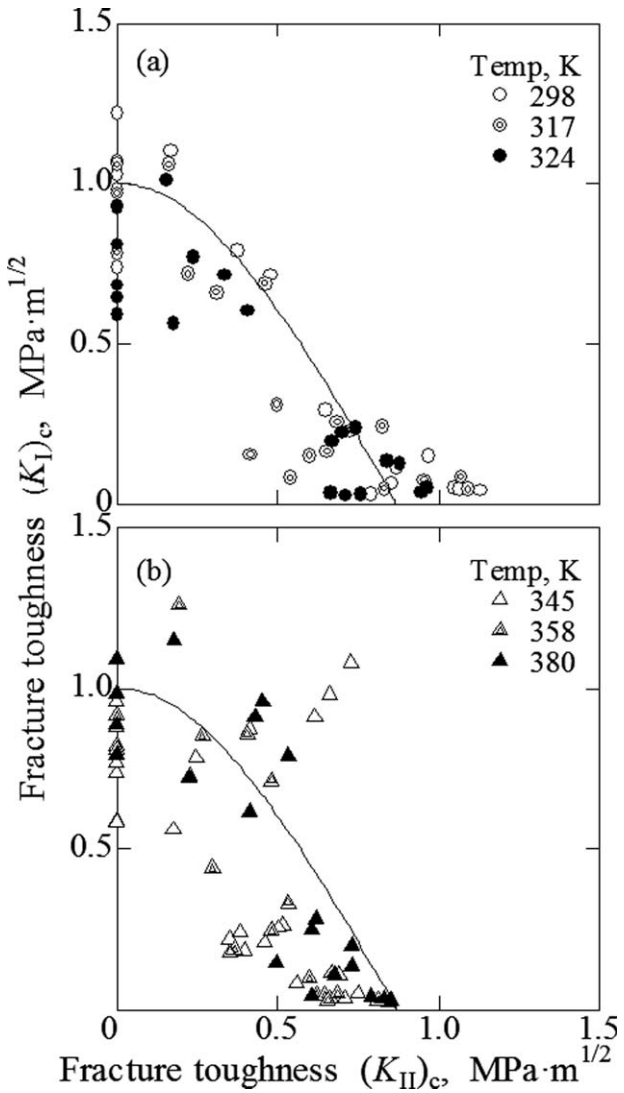

Figure 10 Fracture locus.

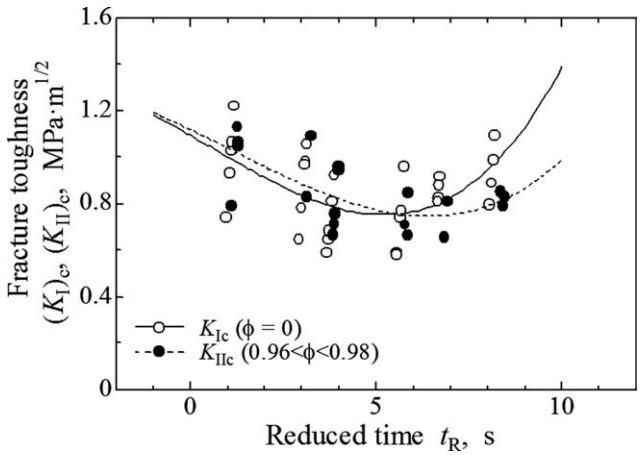

Figure 11 Master curves of fracture toughness with the approximations.

$$K_{IIc} = \alpha_1 K_{Ic}(\beta_1 \tau_{RI} + \beta_2) + \alpha_2 = \alpha_1 K_{Ic}(\tau_{RII}) + \alpha_2 = K_{IIc}(\tau_{RII}), \quad (8)$$

where the constants α_i and β_i calibrate the magnitude and the time-scale of K_{IIc}, respectively. τ_{RI} and τ_{RII} are simply log t_R for K_{Ic} and K_{IIc}, respectively. Particularly in the case of $\alpha_2 = 0$,

$$K_{IIc} = \alpha_1 K_{Ic}(\tau_{RII}) = K_{IIc}(\tau_{RII}). \quad (8a)$$

The ratio K_{IIc}/K_{Ic} is often a very important factor for the conventional fracture criteria.

Figure 11 shows the master curves of K_{Ic} and K_{IIc} with the approximated curves, where K_{Ic} is simply approximated by a cubic function $K_{Ic}(\tau_{RI}) = 1.09 - 0.0918\tau_{RI} - 0.00282\tau_{RI}^2 + 0.00150\tau_{RI}^3$ and K_{IIc} is expressed by eq. (8) with $\alpha_1 = 0.997$, $\alpha_2 = 0$, $\beta_1 = 0.866$, $\beta_2 = -0.358$. The approximated curve of K_{IIc} is well agreed with the experimental data, which means that the master curve of K_{IIc} can be given by magnifying and time-shifting of that of K_{Ic}. In addition, as β_1 and β_2 are calibration factors of the time-scale of mode II to mode I, they can be applicable not only for K_{Ic} and K_{IIc} but also for $(K_I)_c$ and $(K_{II})_c$ with the mode mixity $0 < \phi < 1$.

The fracture criterion should consider the time-temperature dependence of fracture toughness seen in the master curves. The general empirical fracture criterion[23] is given by:

$$\frac{(K_I)_c}{K_{Ic}} + \left(\frac{(K_{II})_c}{CK_{Ic}}\right)^2 = 1 \quad (9)$$

where $C = K_{IIc}/K_{Ic}$. Because eq. (9) does not take account of the time-temperature dependence of the fracture toughness, it can be rewritten as

$$\frac{(K_I)_c(\tau_{RI})}{K_{Ic}(\tau_{RI})} + \left(\frac{(K_{II})_c(\tau_{RI})}{CK_{Ic}(\tau_{RI})}\right)^2 = 1 \quad (10)$$

where $C = K_{IIc}(\tau_{RI})/K_{Ic}(\tau_{RI})$. Considering the time-temperature dependence discussed above, eq. (10) should be revised as:

$$\frac{(K_I)_c(\tau_{RI})}{K_{Ic}(\tau_{RI})} + \left(\frac{(K_{II})_c(\tau_{RII})}{CK_{Ic}(\tau_{RI})}\right)^2 = 1 \quad (11)$$

where the constant $C = K_{IIc}(\tau_{RII})/K_{Ic}(\tau_{RI})$ is equal to α_1 in the present case ($\alpha_2 = 0$).

Application of the proposed criterion

Figure 12 illustrates the fracture locus $(K_I)_c - (K_{II})_c$ based on the concept of eq. (11) for the case of $\tau_{RI} = 8.2$, i.e., the reduced time $t_R = 10^{8.2}$ s, at the reference temperature $T_R = 298$ K. The largest envelope is given by $(K_I)_c(\tau_{RI})$ and $(K_{II})_c(\tau_{RI}) = \alpha_1(K_{II})_c(\tau_{RI})$, whereas the smallest one is given by $(K_I)_c(\tau_{RII})$ and $(K_{II})_c(\tau_{RII}) = \alpha_1(K_{II})_c(\tau_{RII})$. As $(K_{II})_c$ and $(K_{II})_c$ have the different time-scale from each other, the fracture locus should be given by $(K_I)_c(\tau_{RI})$ and $(K_{II})_c$ (τ_{RII}), as shown by the middle envelope.

Figure 13 shows the fracture locus $(K_I)_c - (K_{II})_c$ for $\tau_{RI} = 1.1$–8.2, which are roughly equivalent for the temperatures from 298 to 380 K. The small difference in the reduced fracture time t_R depending on the mode mixity is neglected in this study. The proposed fracture locus given by eq. (11) approximates the experimental date quite well. By using eq. (11), the temperature dependence of the fracture toughness for various modes, e.g., Figures 6 and 7, can be easily determined by this method. As an example of this, the predicted relationship between the mode mixity–fracture toughness at various temperatures is shown in Figure 14. The prediction at $\tau_{RI} = 1.1$ in

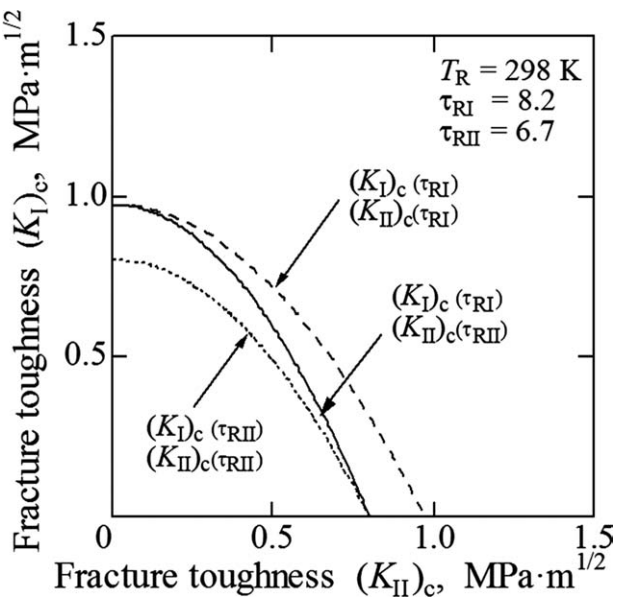

Figure 12 Illustration of the proposed fracture criterion.

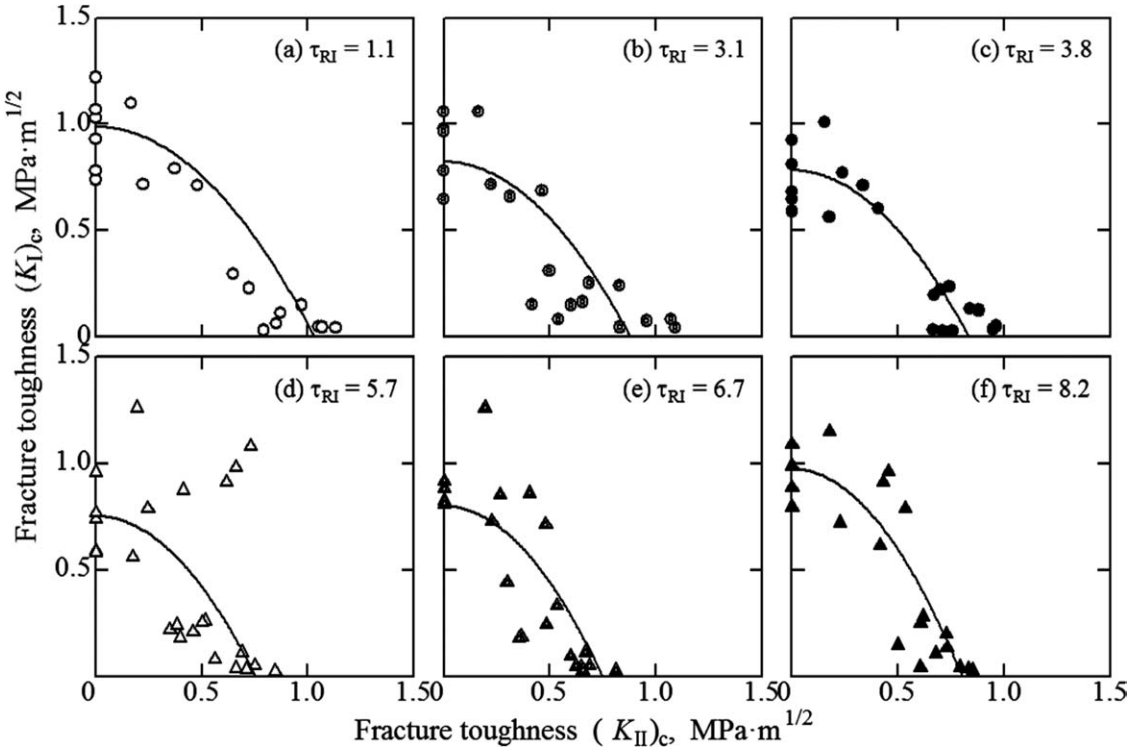

Figure 13 Fracture locus with the prediction by the proposed method.

Figure 14 almost agrees with the experimental results in Figure 6. Therefore, the fracture toughness of the phenolic resin under various conditions of temperature, time, and mode mixity can be predicted by the proposed method.

The present approach, which requires the master curves of the pure mode I an II fracture toughness, will be very useful for predicting fracture toughness of the viscoelastic materials at any temperature, at any rate, and with any mode mixity. The validity of the present approach can be further discussed based on results of various viscoelastic materials.

CONCLUSIONS

In this study, the temperature dependence of the mixed-mode fracture toughness of the phenolic resin for friction materials is investigated.

For pure mode I, the fracture toughness decreases as the temperature increases, and it increases again after showing its minimum value. For pure mode II, the fracture toughness shows the similar trend but has its minimum value at a higher temperature. The temperature dependence of the mixed-mode fracture toughness varies depending on the mode mixity, which is attributed to the different sensitivity to the relaxation phenomenon.

At 298 K, as the fracture toughness for pure mode I and II are almost the same, the fracture locus shows a circular arc. With increasing the temperature, the locus becomes smaller and noncircular. At 380 K, the fracture locus shows an elliptical arc, where the fracture toughness for pure mode II is smaller than that for mode I. These complex behaviors are directly related to the different temperature dependence of the fracture toughness for different mode, which cannot be predicted by the conventional fracture criteria. On the other hand, the crack

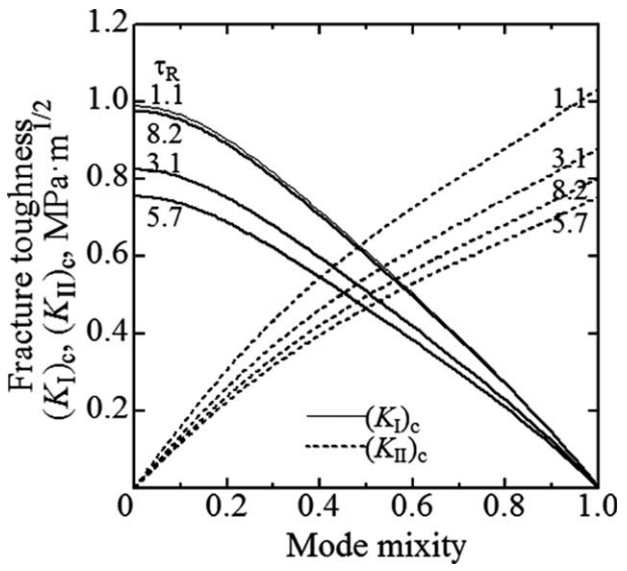

Figure 14 Prediction of mixed mode I/II fracture toughness.

initiation angles are almost consistent regardless of the temperature, which agree with the maximum hoop stress theory.

An empirical fracture criterion that considers the time-temperature dependence of the mixed-mode I/II fracture toughness is proposed based on the experimental results. It is shown that the proposed approach can successfully predict the fracture toughness of the phenolic resin under various conditions of the temperature, time and mode mixity.

References

1. Knop, A.; Pilato, L.A. In Phenolic Resin—Chemistry, Applications and Performance; Springer: Berlin, 1985, Chapter 18.
2. Tanaka, K.; Veda, S. Wear 1973, 23, 349.
3. Barth, B. P.; Skeist, I., Eds. Handbook of Adhesives; van Norstand: NY, 1977, Chapter 23.
4. Schwarzl, F.; Staverman, A. J. J Appl Phys 1952, 23, 838.
5. Buche, F. J Appl Phys 1955, 26, 1133.
6. Smith, T. L. J Polym Sci 1958, 32, 99.
7. Frassine, R.; Rink, M.; Pavan, A.; Frassine, R. Comput Sci Technol 2001, 61, 57.
8. Massa, W.; Piques, R.; Laurent, A. J Mater Sci 1997, 32, 6583.
9. Lim, W. W.; Mizumachi, H. J Appl Polym Sci 1995, 57, 55.
10. Han, Y.; Yang, Y.; Li, B.; Wang, X.; Feng, Z. J Appl Polym Sci 1995, 57, 655.
11. Araki, W.; Adachi, T.; Gamou, M.; Yamaji, A. IMech E Part L 2002, 216, 79.
12. Araki, W.; Adachi, T.; Yamaji, A. J Thermal Stresses 2007, 30, 459.
13. Araki, W.; Asahi, D.; Adachi, T.; Yamaji, A. J Appl Polym Sci 2005, 96, 51.
14. Brown, E. N.; Rae, P. J.; Liu, C. Mech Sci Eng A 2007, 468–470, 253.
15. Wu, C.; Mantell, S. C.; Davidson, J. H. Polym Eng Sci 2006, 48, 2216.
16. Kanchanomai, C.; Rattananon, S. J Appl Polym Sci 2008, 109, 2408.
17. Araki, W.; Nemoto, K.; Adachi, T.; Yamaji, A.; Acta Mater 2005, 53, 869.
18. Hua, G.; Brown, M. W.; Miller, K. J. Fatig Eng Mater Struct 1982, 5, 1.
19. Fett, T. Int J Fract 1991, 48, R67.
20. Fett, T. Theo Appl Fract Mech 1991, 15.
21. Benthem, J. P.; Koiter, W. T.; Sih, G. C., Eds. Methods of Analysis and Solutions of Crack Problems; Noordhoff: Leyden, 1973, Chapter 3.
22. Erdgan, F.; Sih, G. C. Basic Eng 1963, 85, 519.
23. Richard, H. A. VDI Forschungsh 1985, 631, 1.